CHAPTER IV

RESULTS AND DISCUSSIONS

4.1 Determination of counting conditions.

4.1.1 Determination of optimum gain setting of liquid scintillation spectrometer for radon counting.

The results of counting a radon sample at different gain setting are shown in Table 4.1 and plotted in Figure 4.1.

Table 4.1 Variation of count rate as a function of gain.

Conditions :			
	Activities of standard radium-226	1031	Pci
	ingrowth factor	0.9052	
	flow rate of nitrogen	150	$cm^3 mim^{-1}$
	de-emanation time	50	minutes
	particle size of silica gel	30-70	mesh
	weight of silica gel	2.5	g
	warm up time	5	minutes
	warm up temperature	0	^{o}c
	volume of liquid scintillator	15	cm^3
	desorption temperature	30	^{c}c
	Counting time	4	minutes

gain%	count rate of standard Ra-226 (cpm)	Background count rate (cpm)	Net Count rate of standard (cpm)
0.2	3394.3	23.3±2.4*	3371.0
0.4	4229.9	31.9±2.8	4198.0
0.6	4861.8	39.3±3.1	4822.5
0.8	5018.3	47.8±3.4	4970.5
1.0	5372.5	57.5±3.8	5315.0
1.2	5300.9	56.9±3.8	5244.0
1.4	5408.3	57.8±3.8	5350.5
1.6	4886.9	55.9±3.7	4831.0
1.8	4753.9	53.8±3.7	4700.0
2.0	4494.1	50.1±3.5	4444.0
3.0	2372.0	19.5±2.2	2352.5
4.0	1975.8	17.3±2.1	1958.5
5.0	1757.8	16.8±2.0	1741.0
6.0	1582.3	16.3±2.0	1566.0
7.0	1460.5	13.0±1.8	1447.5
8.0	1297.3	12.3±1.7	1285.0
9.0	1168.9	11.9±1.7	1157.0
10.0	1071.9	9.9±1.5	1062.0

* Standard deviation $= \sqrt{\frac{N}{T}}$ where N = total count and T = Counting time

From the results above, the maximum count rate is therefore obtained by setting the gain of the scintillation counter at 1 per cent

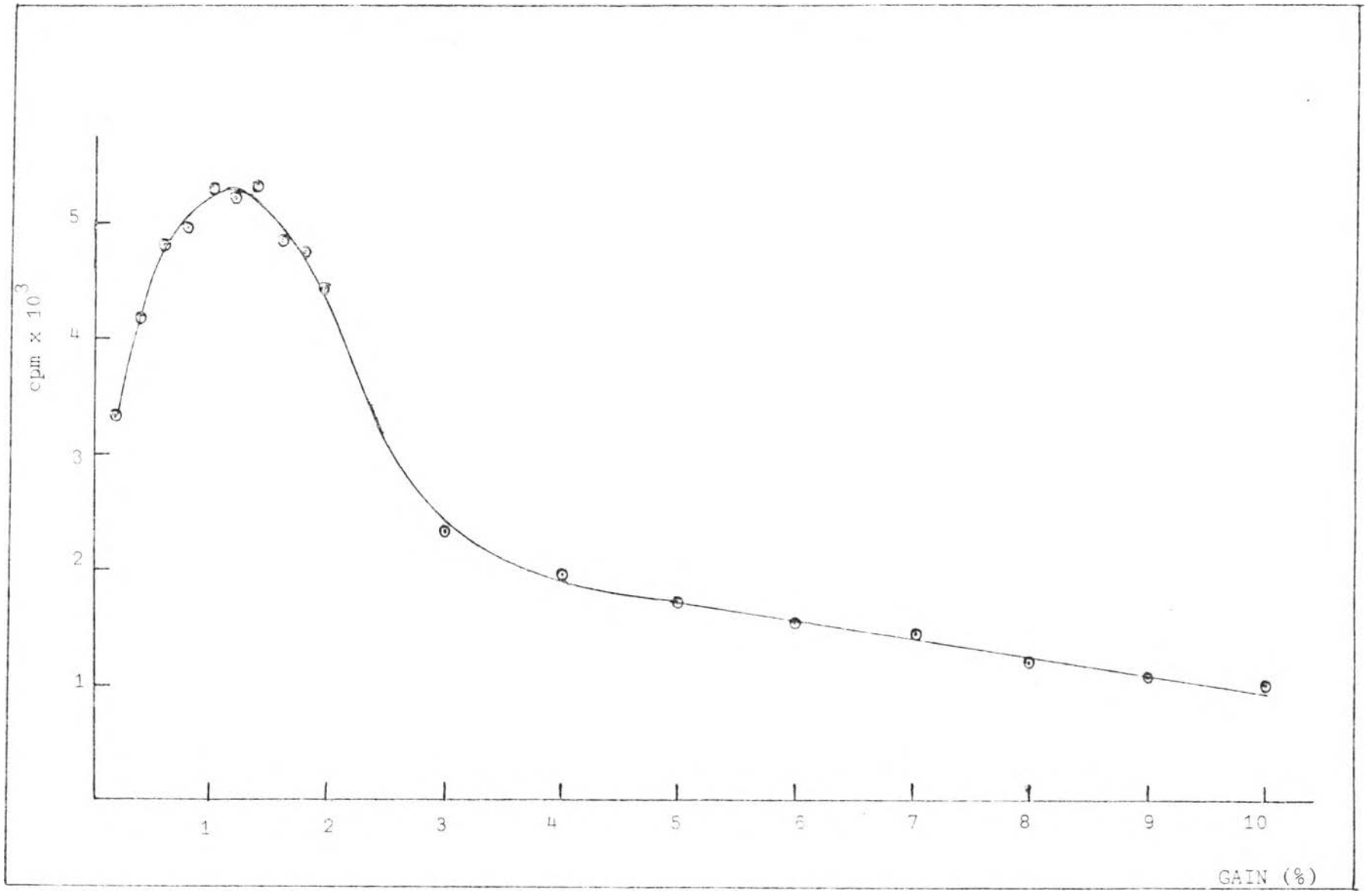

Figure 4.1 Variation of the count rate as a function of gain

4.1.2 The determination of discrimination levels for radon counting.

The viriation of count rate as a function of discriminator levels was studied by counting the sample prepared under section 4.1.1. The gain of the spectrometer was set at the optimum of 1 per cent. The results are tabulated in Table 4.2 and graphically shown in Figure 4.2.

Table 4.2 Variation of count rate as a function of discriminator levels.

Conditions :	Activities of standard radium-226	1031	Pci
	ingrowth factor	0.9052	
	flow rate of nitrogen	150	$cm^3 min^{-1}$
	de-emanation time	50	minutes
	particle size of silica gel	35-70	mesh
	weight of silica gel	2.5	g
	warm up time	5	minutes
	warm up temperature	0	°c
	volume of liquid scintillator	15	cm^3
	desorption temperature	30	°c
	counting time for sample	4	minutes
	counting time for background	20	minutes

discriminator levels	Count rate of standard Ra-226 (cpm)	Background count rate (cpm)	Net count rate of standard (cpm)
0-50	461.5	20.5±1.0	441.0
50-100	577.7	13.2±0.8	564.5
100-150	501.0	9.0±0.7	492.0
150-200	300.8	6.3±0.6	294.5
200-250	250.8	3.8±0.7	247.0
250-300	244.5	4.5±0.5	240.0
300-350	472.3	1.3±0.2	471.0
350-400	819.7	0.7±0.2	819.0
400-450	817.3	0.8±0.2	816.5
450-500	418.9	0.9±0.2	418.0
500-550	177.0	1.0±0.2	176.0
550-600	178.9	0.4±0.1	178.5
600-650	289.8	0.3±0.1	289.5
650-700	380.8	0.8±0.2	380.0
700-750	257.7	0.7±0.2	257.0
750-800	50.6	1.1±0.2	49.5
800-850	43.5	1.0±0.2	42.5
850-900	31.8	2.3±0.3	29.5
900-950	21.8	3.3±0.4	18.5
950-1000	21.1	4.1±0.4	17.0

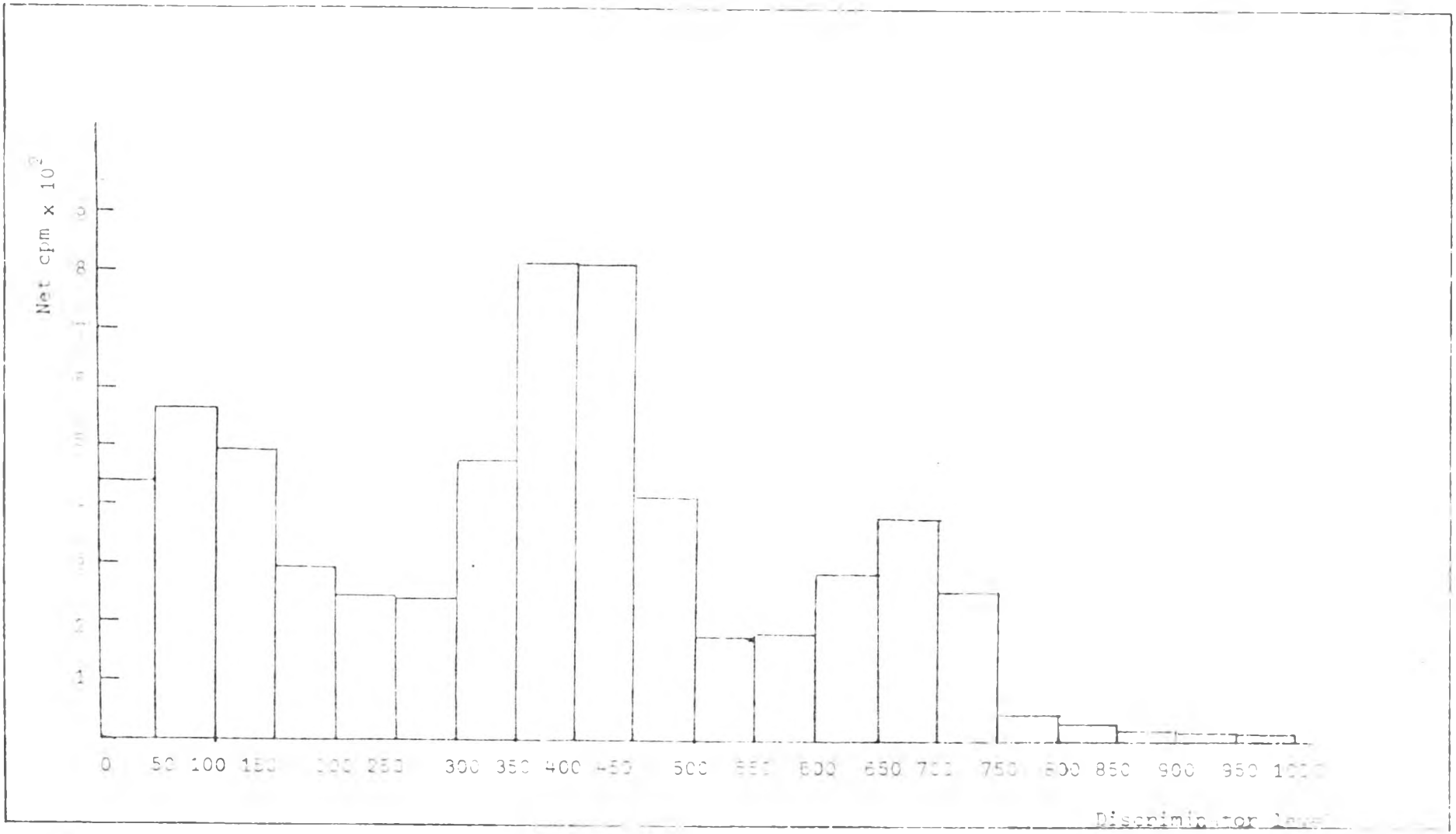

Figure 4.2 Variation of count rate as a function of discriminator levels.

The best conditions for counting is obtained when the figure of merit or the function $(\text{efficiency})^2/\text{background}$ is at a maximum. (17) Table 4.3 shows the figure of merit obtained by setting the discriminators at various levels.

Table 4.3 Figure of Merit at various discriminator levels.

Discriminator		Count rate of standard Ra-226 (cpm)	Background count rate (cpm)	Net count rate of standard (cpm)	Efficiency (cpmPci^{-1})	E^2/Bg
lower level	Upper level					
0	1000	6317.5	76.0±2.0	6241.5	6.69	48.64
50	1000	5856.0	55.5±1.7	5800.5	6.22	57.52
300	650	3173.9	5.4±0.5	3168.5	3.40	176.41
300	800	3863.0	8.0±0.6	3855.0	4.13	176.26
300	1000	3981.2	18.7±1.0	3962.5	4.24	79.67

If the three alpha-particles and the two beta-particles were counted with 100 per cent efficiency, 11 counts $min^{-1}Pci^{-1}$ would be the maximum attainable over-all efficiency. In practice, when the gain and discriminator controls of the liquid scintillator spectrometer are set to detect the maximum number of particles, the highest efficiency observed is 6.69 counts $min^{-1}Pci^{-1}$ of radon. At these discriminator settings (0-1000) the background is, however, high at 76.0±2.0 counts min^{-1}. The discrimination levels between 300-650 were chosen. At these optimum discriminator settings the over-all efficiency is 3.40 counts min^{-1} Pci^{-1} of radon and the background is 5.4 ± 0.5 counts min^{-1}.

4.2 Determination of time required for establishment of equilibrium between radon and its daughters.

The activity of a radon sample counted at different time are given in Table 4.4 and graphically illustrated in Figure 4.3.

Table 4.4 Variation of count rates as a function of decay time after de-emanation.

Conditions :			
	Activities of radium-226 standard Solution	104	Pci
	ingrowth factor	0.7185	
	flow rate of nitrogen gas	150	$cm^3 min^{-1}$
	de-emanation time	50	minutes
	particle size of silica gel	35-70	mesh
	weight of silica gel	2.5	g
	warm up time	5	minutes
	warm up temperature	0	°c
	volume of liquid scintillator	15	cm^3
	desorption temperature	30	°c
	gain	1	per cent
	discriminator levels	300-650	
	counting time	20	minutes

decay time after de-emanation (min)	count rate of standard Ra-226 (cpm)	Background count rate (cpm)	Net count rate of standard (cpm)
20	189.6	3.1±0.4	186.5
40	222.7	2.5±0.3	220.2
60	235.6	3.8±0.4	231.8
80	256.3	4.3±0.5	252.0
100	269.3	4.0±0.4	265.3
120	283.4	4.5±0.5	278.9
140	274.0	4.5±0.5	269.5
160	281.4	4.0±0.4	277.4
180	284.3	4.8±0.5	279.5
200	285.3	5.0±0.5	280.3
220	286.3	5.1±0.5	281.2
240	284.3	5.3±0.5	279.0
260	282.1	5.2±0.5	276.9
280	286.0	5.0±0.5	281.0
300	283.7	5.2±0.5	278.5
320	281.0	5.1±0.5	275.9

From Figure 4.3, it is obvious that radioactive equilibrium is established within 3 hours after de-emanation.

In order to confirm that a pure radon sample was obtained from the de-emanation, a sample of 111 Pci Ra-226 was de-emanated and the radon sample obtained was counted after the radicactive equilibrium

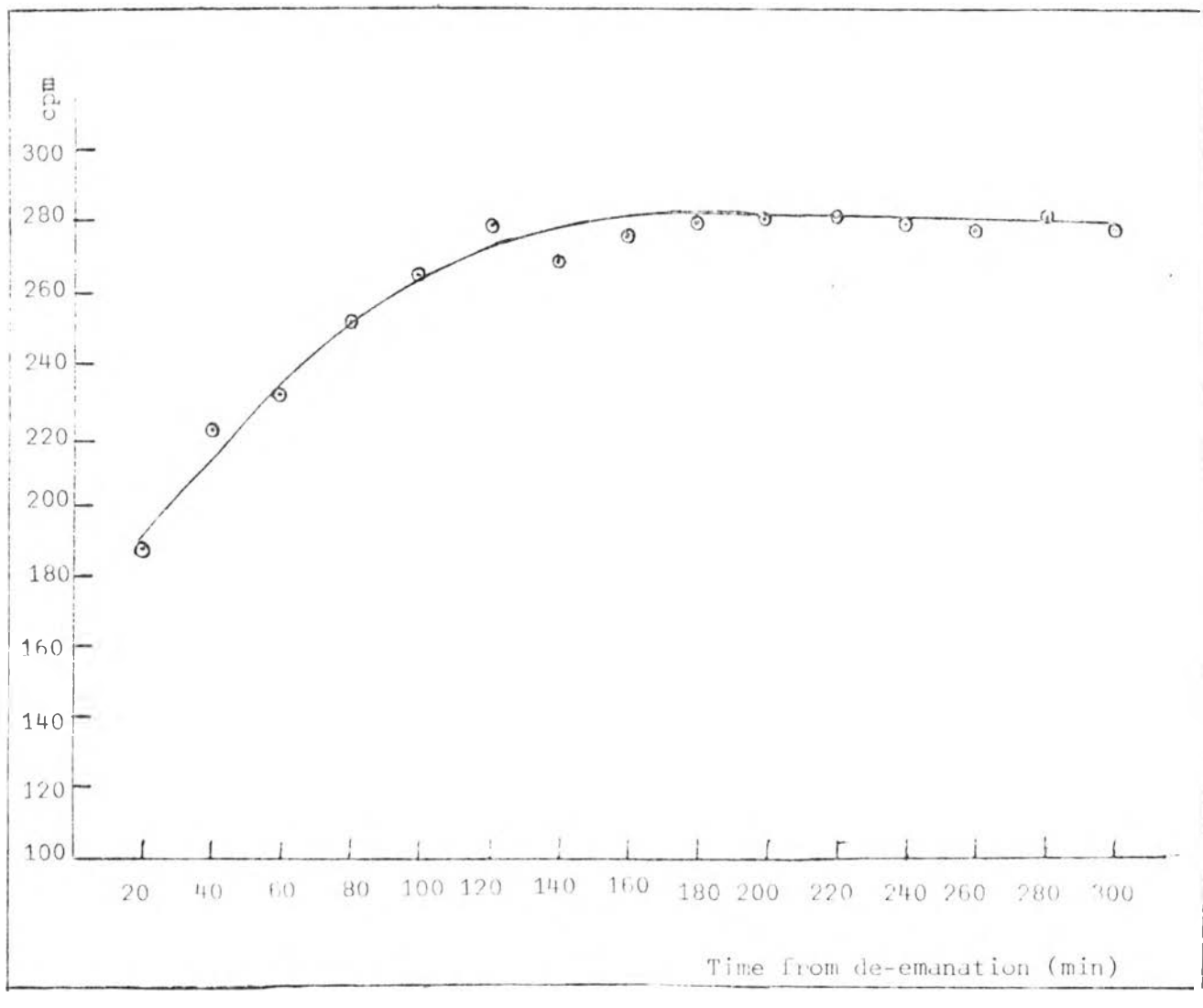

Figure 4.3 Ingrowth of radon-222

between radon and its daughters had been established.

The results and the decay curve are shown in Table 4.5 and Figure 4.4 respectively

Table 4.5 Count rate as a function of decay time.

Conditions :			
	Activities of standard radium 226	111	Pci
	ingrowth factor	0.5156	
	flow rate of nitrogen	150	$cm^3 min^{-1}$
	de-emanation time	50	minutes
	particle size of silica gel	35-70	mesh
	weight of silica gel	2.5	g
	warm up time	5	minutes
	warm up temperature	0	°c
	volume of liquid scintillator	15	cm^3
	desorption temperature	30	°c
	counting time	20	minutes

decay time after de-emanation (hr)	Count rate of standard Ra-226 (cpm)	Background count rate (cpm)	Net count rate of standard (cpm)
4.16	183.3	5.2±0.5	178.1
29.33	162.7	5.0±0.5	157.7
58.16	127.7	4.6±0.4	123.1
76.58	213.4	4.0±0.4	109.4
143.16	70.9	3.5±0.4	67.4
167.58	57.8	3.3±0.4	54.5
176.42	55.3	3.5±0.4	52.1
181.50	52.2	3.2±0.4	49.0
193.33	45.5	3.1±0.4	42.4

From the decay curve, an approximate half-life of 92 hours was abtained which was in good agreement with the half-life of radon-222.

4.3 Determination of de-emanation conditions.

4.3.1 Effect of de-emanation time on efficiency.

The efficiency; or the specific count rate, obtained at different de-emanation times when the nitrogen gas flow rate was varied between 100 and 250 $cm^3 min^{-1}$ is given in Table 4.6 and graphically shown in Figure 4.5

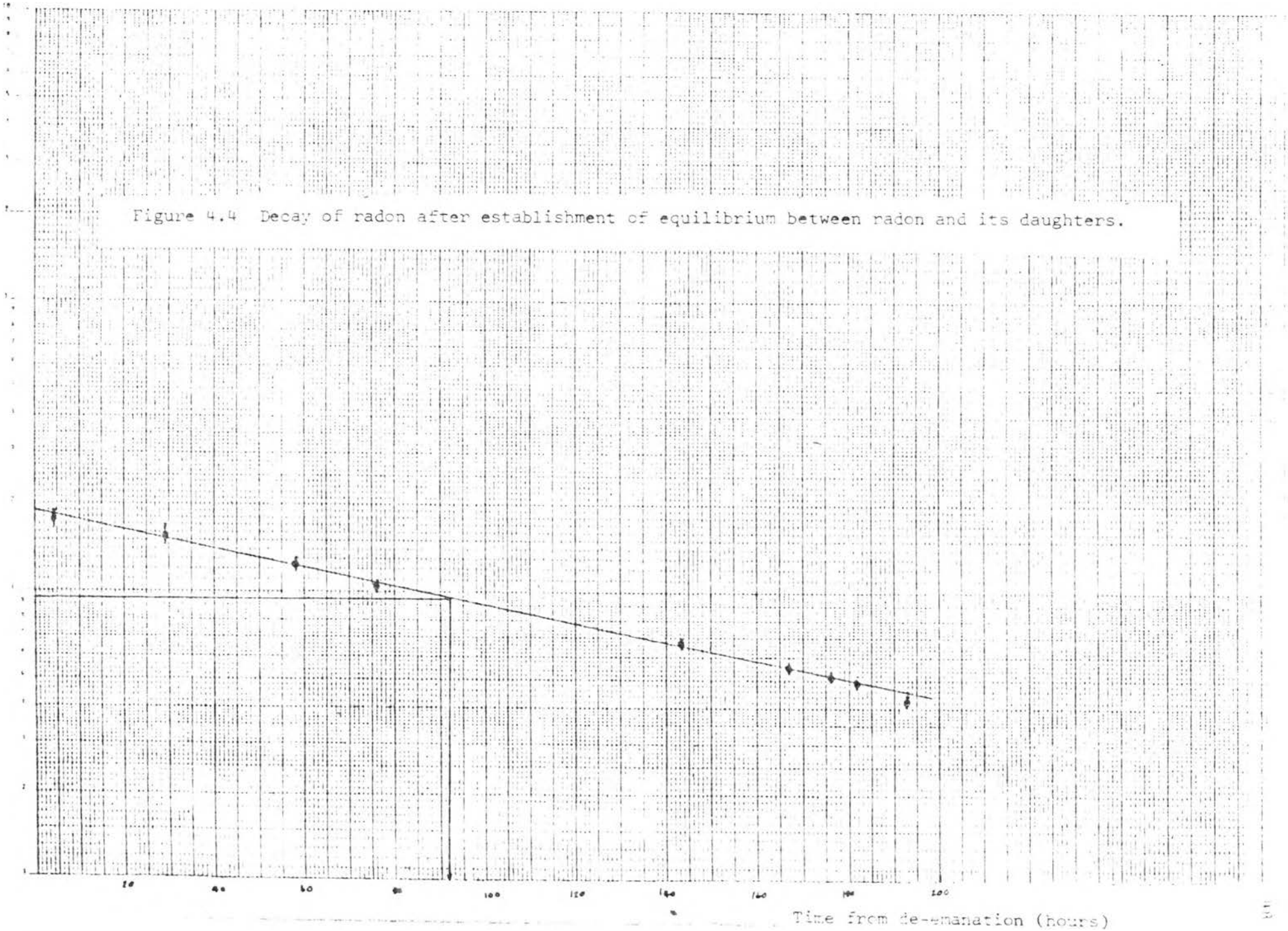

Figure 4.4 Decay of radon after establishment of equilibrium between radon and its daughters.

Table 4.6 Effect of de-emanation time on efficiency at nitrogen flow rate between 100 and 250 $cm^3 min^{-1}$

conditions :	Activities of standard radium 226	263	Pci
	flow rate of nitrogen gas	100-250	$cm^3 min^{-1}$
	particle size of silica gel	35-70	mesh
	weight of silica gel	2	g
	warm up time	5	minutes
	warm up temperature	0	°c
	volume of liquid scintillator	15	cm^3
	desorption temperature	30	°c
	counting time	100	minutes

V_{N_2} gas / Vde-emanation	De-emanation time (min)	Efficiency (cpmPci^{-1})			
		Expt.1	Expt.2	Expt.3	Average
nitrogen flow rate 100 cm^{3}min^{-1}					
5	15	2.30	2.35	2.16	2.27±0.09
10	30	2.66	2.87	2.75	2.76±0.11
15	45	3.33	3.43	3.73	3.51±0.19
20	60	3.43	3.48	3.54	3.48±0.06
30	90	3.88	3.69	3.40	3.66±0.24
nitrogen flow rate 150 cm^{3}min^{-1}					
5	10	2.22	2.17	2.20	2.19±0.02
10	20	2.60	2.64	2.70	2.65±0.05
15	30	3.49	3.61	3.75	2.62±0.13
22.5	45	3.38	3.35	3.34	3.36±0.02
30	60	3.44	3.56	3.50	3.50±0.06
nitrogen flow rate 250 cm^{3}min^{-1}					
5	6	2.08	2.23	2.33	2.21±0.13
10	12	2.88	2.76	2.81	2.82±0.06
15	18	3.69	3.32	3.80	3.60±0.25
20	24	3.60	3.75	3.50	3.62±0.13
30	36	3.85	3.76	3.63	3.75±0.11

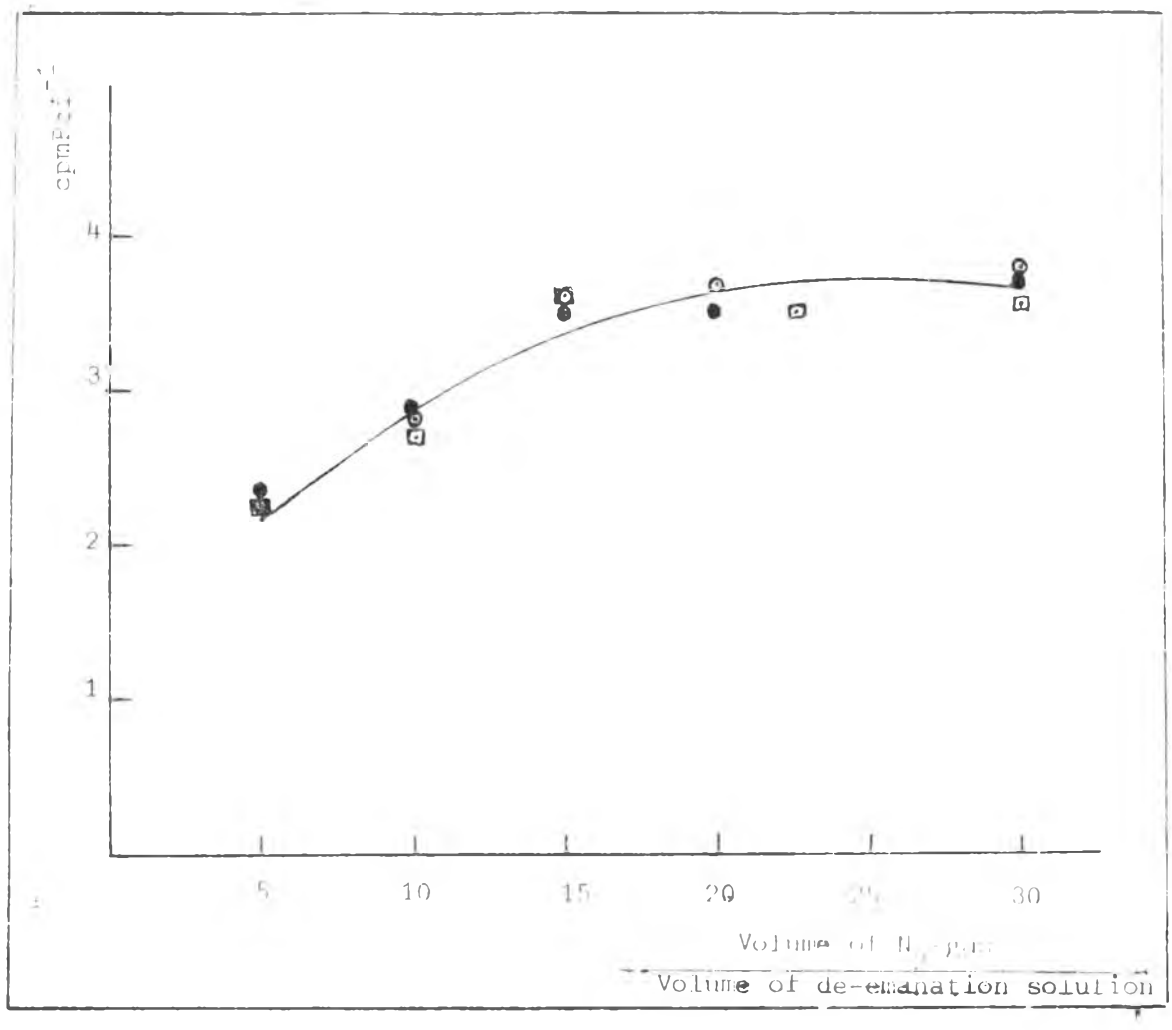

Figure 4.5 Effect of de-emanation time on efficiency at nitrogen flow rate between 100 and 250 $cm^3 min^{-1}$

● : nitrogen flow rate of 100 $cm^3 min^{-1}$

▣ : nitrogen flow rate of 150 $cm^3 min^{-1}$

⊙ : nitrogen flow rate of 250 $cm^3 min^{-1}$

From the results it is seen that, a maximum efficiency was obtained at approximately 3.57±0.18 cpmPci^{-1} when a volume of nitrogen gas equals to 15 times that of the de-emanation solution has been passed. No difference was observed when the flow rate was varied between 100 and 250 cm^{3}min^{-1}.

4.3.2 Effect of nitrogen flow rate on efficiency.

The influence of nitrogen flow rate was investigated by fixing the volume of gas at 15 times that of the volume of the de-emanation solution. The results of the investigation are shown in Table 4.7

Table 4.7 Effect of nitrogen flow rate on efficiency at a ratio of 15 between the volume of nitrogen to the volume of the de-emanation solution

conditions : conditions were similar to those described under section 4.3.1

Nitrogen flow rate (cm^{3}min^{-1})	De-emanation time (min)	Efficiency (cpmPci^{-1})			
		Expt.1	Expt.2	Expt.3	Average
100	45	3.38	3.43	3.73	3.51±0.19
150	30	3.49	3.61	3.75	3.61±0.13
250	18	3.69	3.32	3.80	3.60±0.25
300	15	3.59	3.38	3.50	3.49±0.10
400	11.25	2.51	2.66	2.57	2.57±0.08

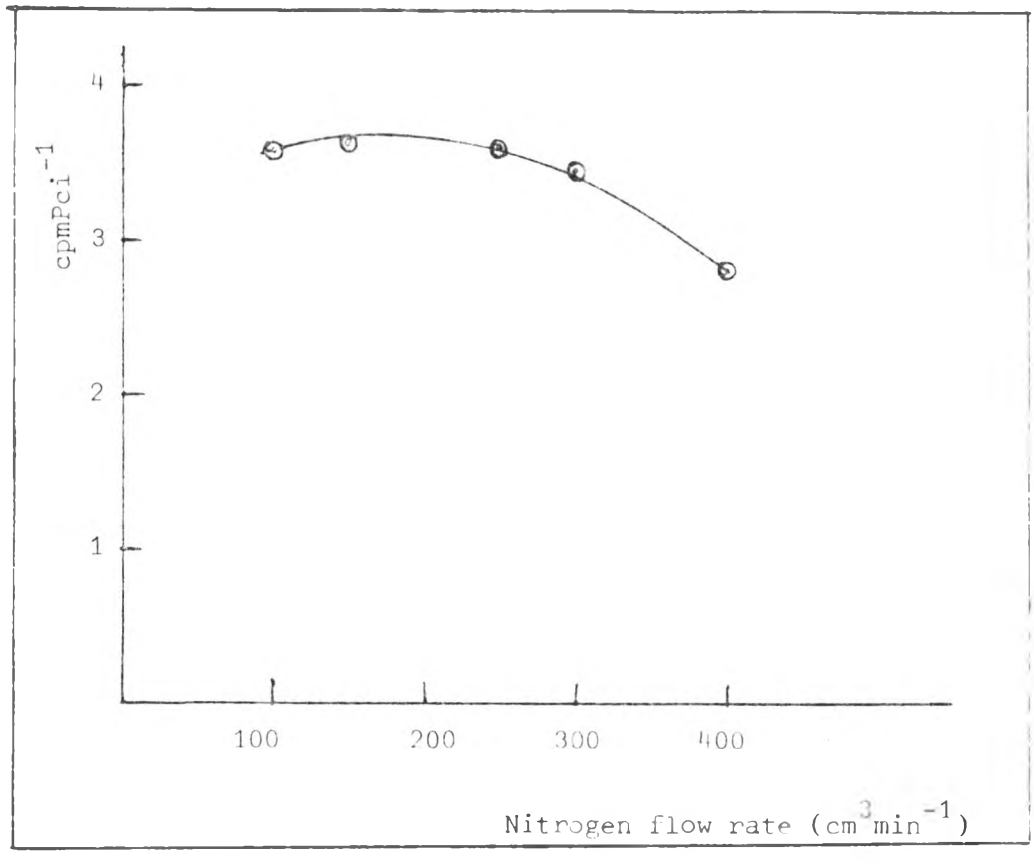

Figure 4.6 Effect of nitrogen flow rate on efficiency at a ratio of 15 between the volume of nitrogen to the volume of de-emanation solution.

The effect of nitrogen flow rate on efficiency is graphically shown in Figure 4.6. A constant efficiency of 3.57 ± 0.18 cpmPci^{-1} was obtained when the gas flow-rate was under 300 cm^{3}min^{-1}. Further increase of the flow resulted in a decrease in the efficiency. At high nitrogen flow-rate the particles of silica gel moved inside the [illegible] trap and radon could not be adsorbed quantitatively.

The results of the present investigation support the results obtained by Jacobi (30) which indicated that radon might be effectively swept out of an aqueous solution at room temperature provided that the sweeping gas passed through the solution as a stream of small bubbles, and the total volume of gas was large compared with the volume of the de-emanation solution. This, however, disagreed with the result of Moran and Evan (10) which showed that the quantitative removal of radon from an aqueous solution could be achieved by prolonged boiling only.

4.3.3 Effect of particle size of silica gel on efficiency.

The results of the investigation are given in Table 4.8

Table 4.8 Effect of particle size of silica gel on efficiency.

conditions:	Activities of standard radium-226	263	Pci
	flow rate of nitrogen	150	$cm^3 min^{-1}$
	de-emanation time	30	minutes
	weight of silica gel	2	g
	warm up time	5	minutes
	warm up temperature	0	^{o}c
	desorption temperature	30	^{o}c
	volume of liquid scintillator	15	cm^3

particle size of silica gel (mesh)	Efficiency ($cpmPci^{-1}$)			
	Expt.1	Expt.2	Expt.3	Average
16-30	3.66	3.48	3.03	3.39±0.32
35-70	3.49	3.61	3.75	3.62±0.13
85-200	2.61	2.19	2.23	2.01±0.71

According to Darral et. al. (17) the particle size of silica gel should be small enough to permit 100 per cent adsorption of radon but large enough to be stable (not flowing) at high nitrogen flow rate and could be easily transferred. The obtained results from this study indicated that the particle size of 85-200 mesh was too small. However, the difference between 16-30 and 35-70 mesh was not significant. Hence, in the subsequent experiments, the particle size of 35-70 mesh was chosen.

4.3.4 Effect of weight of silica gel on efficiency.

The result of the effect of weight of silica gel used as radon adsorber is shown in Table 4.9 and the efficiency as a function of weight is also plotted in Figure 4.7. The results indicated that, increasing the weight of silica gel from 1.0 to 2.0 g increased the efficiency to a maximum of 3.62 cpmPci^{-1}. Further increase of the weight of adsorber gave a decrease in effciency. Since silica gel did not dissolve in liquid Scintillator; two layers would be formed in the counting vial. The liquid scintillator with all the dissolved radon (31) would be in the upper layer. Apparently, when the weight of silica gel was increased to more than 2 g, the scintillator layer is above the optimum geometry. Consequently, this made a decrease in the efficiency.

Table 4.9 Effect of weight of silica gel on efficiency.

Conditions :	Activities of standard radium-226	263	Pci
	flow rate of nitrogen	150	$cm^3 min^{-1}$
	de-emanation time	30	minutes
	particle size of silica gel	35-70	mesh
	warm up time	5	minutes
	warm up temperature	0	$^{\bullet}c$
	volume of liquid scintillator	15	cm^3
	dessorption temperature	30	$^{\bullet}c$

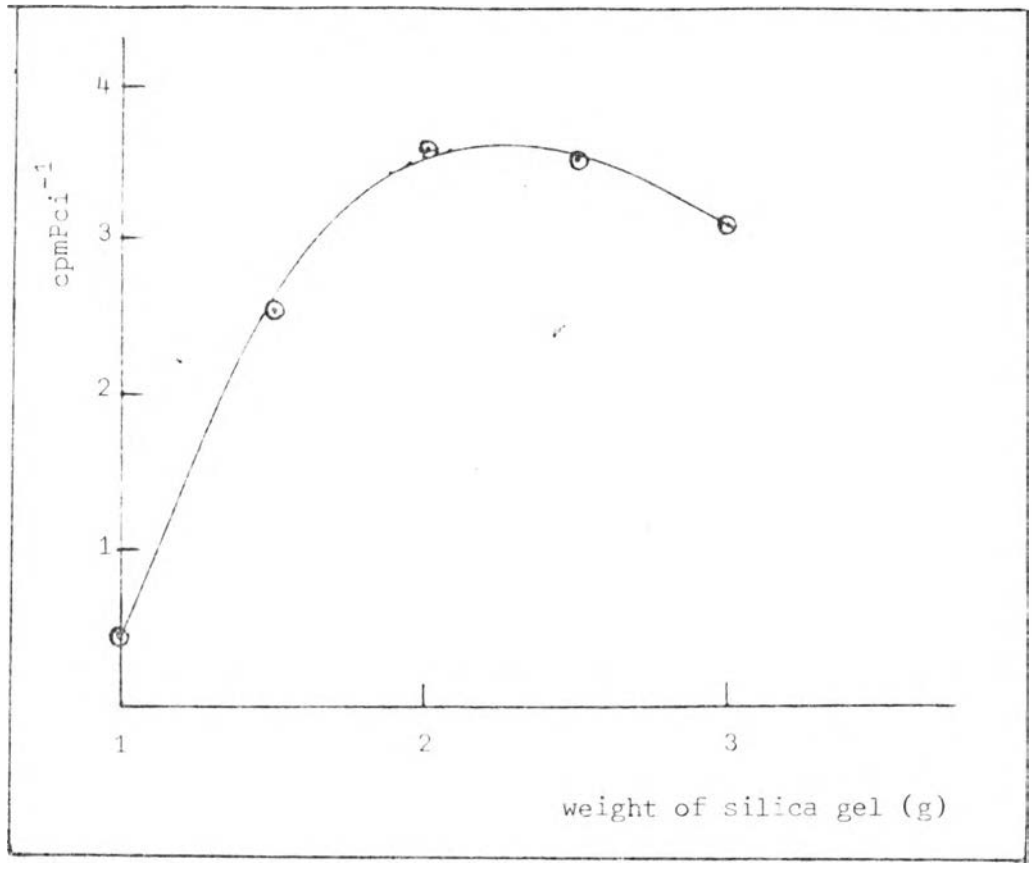

Figure 4.7 Effect of weight of silica gel on efficiency.

weight of silica gel (g)	Efficiency ($cpmPci^{-1}$)			
	Expt.1	Expt.2	Expt.3	Average
1.0	0.51	0.47	0.42	0.47±0.05
1.5	2.64	2.41	2.51	2.52±0.12
2.0	3.49	3.61	3.75	3.62±0.13
2.5	3.43	3.80	3.46	3.56±0.21
3.0	3.11	3.02	3.22	3.12±0.10

4.3.5 Effect of warm up time on efficiency.

The effect of warm up time on efficiency is given in Table 4.10 and graphically shown in Figure 4.8. No significant increase in efficiency was observed when the warm up time was kept longer than 5 minutes.

Table 4.10 Effect of warm up time on efficiency.

Conditions :	Activities of standard radium 226	263	Pci
	flow rate of nitrogen	150	cm^3min^{-1}
	de-emanation time	30	minutes
	particle size of silica gel	35-70	mesh
	weight of silica gel	2	g
	warm up temperature	0	°c
	volume of liquid scintillator	15	cm^3
	desorption temperature	30	°c

warm up time (min)	Efficiency ($cpmPci^{-1}$)			
	Expt.1	Expt.2	Expt.3	Average
0	2.70	2.93	2.77	2.80±0.12
5	3.49	3.61	3.75	3.62±0.13
10	3.12	3.61	3.49	3.41±0.26
20	3.98	3.42	3.37	3.59±0.34

4.3.6 Effect of warm up temperature on efficiency.

The results are given in Table 4.11 and graphically shown in Figure 4.9. It is found that the efficiency decreases at higher temperature. This might happen as a result of the release of radon from the adsorber at higher temperature.

Table 4.11 Effect of warm up temperature on efficiency.

Conditions :	Activities of standard radium-226	263	Pci
	flow rate of nitrogen	150	$cm^3 min^{-1}$
	de-emanation time	30	minutes
	particle size of silica gel	35-70	mesh
	weight of silica gel	2	g
	warm up time	5	minutes
	volume of liquid scintillator	15	cm^3
	desorption temperature	30	^oc

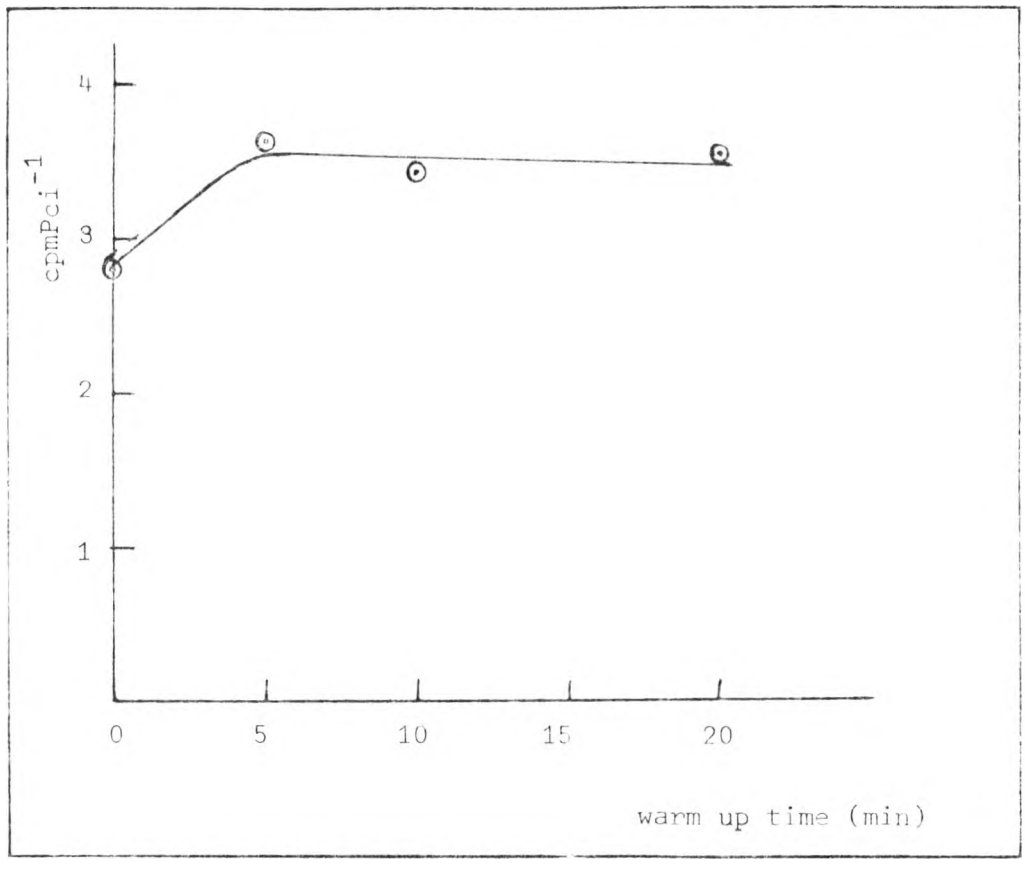

Figure 4.8 Effect of warm up time on efficiency.

warm up temperature (c)	Efficiency ($cpmPci^{-1}$)			
	Expt.1	Expt.2	Expt.3	Average
0	3.49	3.61	3.75	3.62±0.13
15	3.53	3.11	3.47	3.37±0.23
30	2.99	3.18	2.68	2.95±0.25
50	2.71	2.71	3.14	2.85±0.25

4.3.7 Effect of volume of liquid scintillator on efficiency.

The results of the investigation are tabulated in Table 4.12 and the efficiency as a function of volume of liquid scintillator is plotted in Figure 4.10. The results indicated that, increasing the volume of liquid scintillator from 10 to $15cm^3$ increases the efficiency to 3.62 $cpmPci^{-1}$. Further increase of liquid scintillator causes no significant change in efficiency

Table 4.12 Effect of volume of liquid scintillator on efficiency.

Conditions :	Activities of standard radium-226	269	Pci
	flow rate of nitrogen	150	cm^3min^{-1}
	de-emanation time	30	minutes
	particle size of silica gel	35-70	mesh
	weight of silica gel	2	g
	warm up time	5	minutes
	warm up temperature	0	°c
	desorption temperature	30	°c

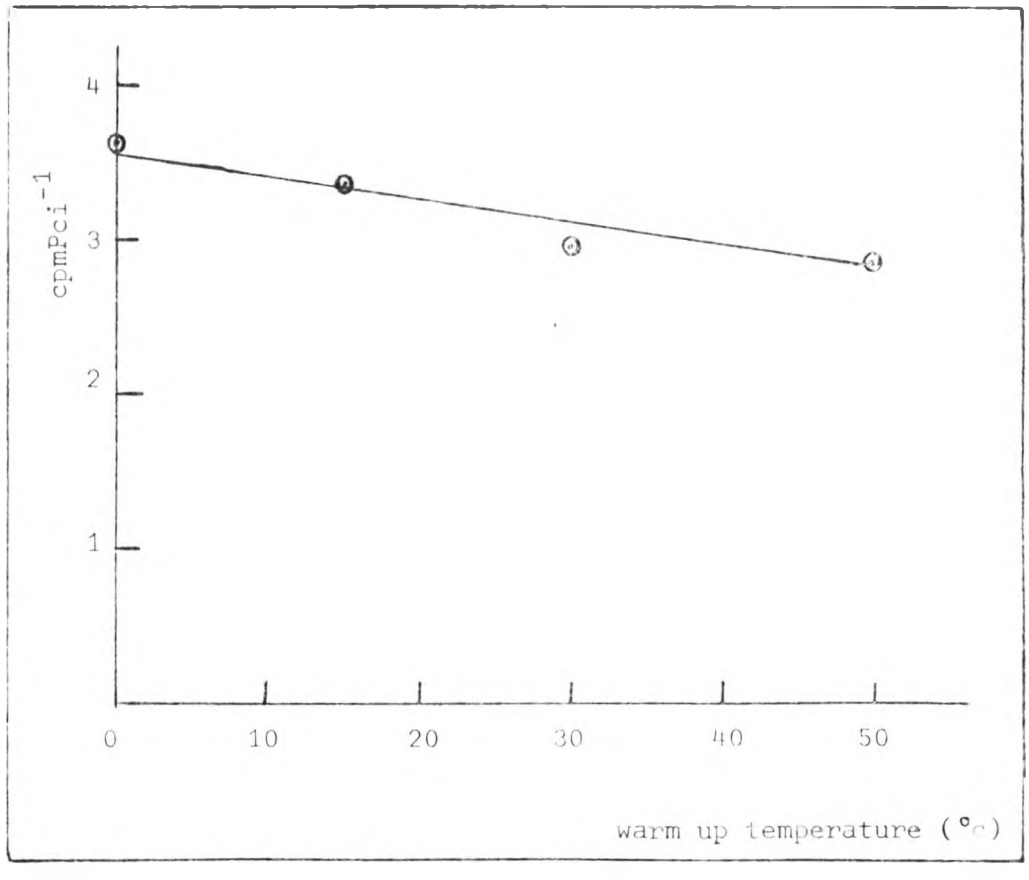

Figure 4.9 Effect of warm up temperature on efficiency.

volume of liquid scintillator (cm^3)	Efficiency ($cpmPci^{-1}$)			
	Expt.1	Expt.2	Expt.3	Average
10	1.35	1.62	1.75	1.57±0.22
13	2.87	2.60	2.85	2.77±0.15
15	3.49	3.61	3.75	3.62±0.13
18	3.72	3.69	3.89	3.77±0.11

4.3.8 Effect of desorption temperature on efficiency.

The results are given in Table 4.13 and graphically shown in Figure 4.11. It is obvious that the count rate is independent on the desorption temperature.

Table 4.13 Effect of desorption temperature on efficiency.

Conditions :	Activities of standard radium 226	263.	Pci
	flow rate of nitrogen	150	$cm^3 min^{-1}$
	de-emanation time	30	minutes
	particle size of silica gel	35-70	mesh
	weight of silica gel	2	g
	warm up time	5	minutes
	warm up temperature	.0	°c
	volume of liquid scintillator	15	cm^3

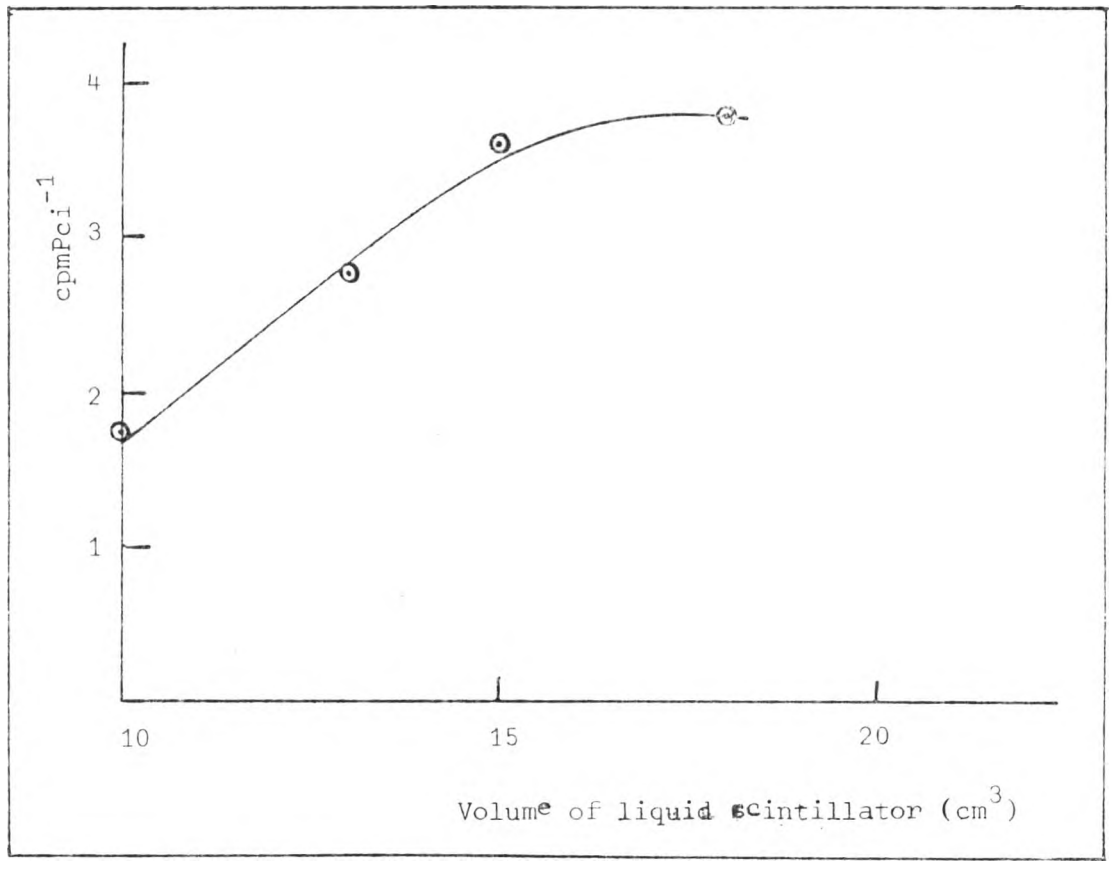

Figure 4.10 Effect of volume of liquid scintillator on efficience.

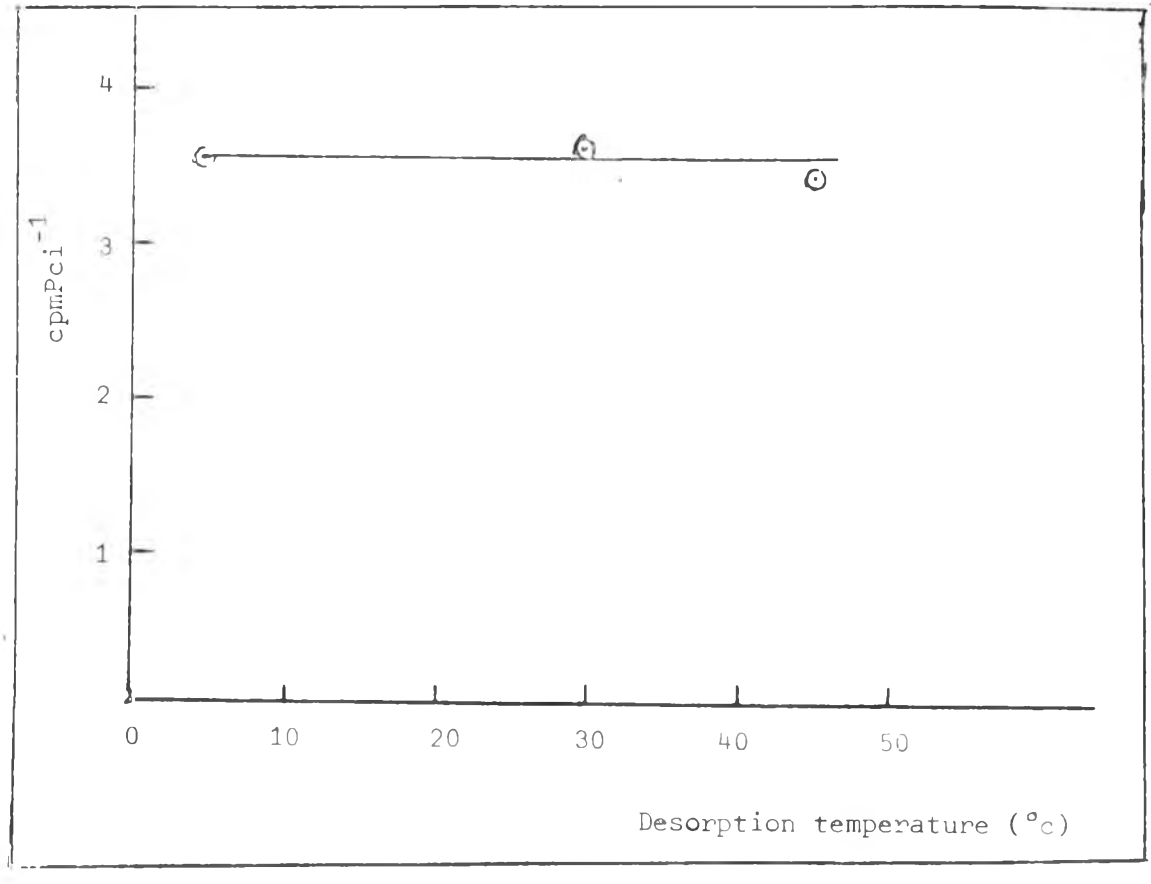

Figure 4.11 Effect of desorption temperature on efficiency.

Desorption temperature (°c)	Efficiency ($cpmPci^{-1}$)			
	Expt.1	Expt.2	Expt.3	Average
4	3.35	3.63	3.49	3.55±0.07
30	3.49	3.61	3.75	3.62±0.15
50	3.55	3.45	3.39	3.46±0.08

The optimum conditions for de-emanation and counting of radon are summarized in Table 4.14.

Table 4.14 Optimum conditions for de-emanation and counting of radon.

flow rate of nitrogen	150	$cm^3 min^{-1}$
de-emanation time	30	minutes
particle size of silica gel	35-70	mesh
weight of silica gel	2	g
warm up time	5	minutes
warm up temperature	0	°c
volume of liquid scintillator	15	cm^3
Desorption temperature	30	°c
gain	1	per cent
discriminator levels	300-650	

4.4 Determination of detection limit.

Standard radium-226 solutions of various activities were prepared. After de-emanation under the optimum conditions as listed in Table 4.13., their activities were measured and the specific activity or efficiency, E.

was evaluated. The results are shown in Table 4.15. The content of radium which gives a specific count rate deviated from 3.50±0.12 $cpmpci^{-1}$ was considered to be outside the dynamic range of the detection.

Table 4.15 Detection limit.

Conditions : as summarized in Table 4.14

standard radium-226 activity (Pci)	Efficiency ($cpmPci^{-1}$)			
	Expt.1	Expt.2	Expt.3	Average
0.50	3.00	2.68	2.39	2.69±0.31
0.70	3.18	2.90	2.63	2.91±0.27
1.1	3.28	3.67	3.79	3.58±0.27
3.2	3.52	3.36	3.80	3.56±0.22
5.2	3.34	3.65	3.19	3.39±0.23
10.4	3.19	3.51	3.46	3.39±0.17
31.2	3.34	3.53	3.48	3.45±0.10
52.0	3.17	3.43	3.29	3.30±0.13
72.8	3.13	3 48	3.53	3.38±0.22
104.0	3.75	3.63	3.50	3.63±0.13
263.0	3.49	3.61	3.75	3.63±0.11
520.0	3.65	3.72	3.51	3.63±0.11
728.0	3.58	3.49	3.71	3.59±0.11

A constant efficiency of 3.50±0.12 $cpmPci^{-1}$ was obtained from a radium activity ranged between 1.1-728 Pci. Lower contents of radium-226 gave significantly lower efficiency. For the developed

method, a detection limit of 1 Pci could be assumed.

4.5 Determination of content of radium-226 in standard uranium ore.

The accuracy of the method was determined by analysing the total radium-226 contents in a standard uranium ore with different sample weights. The results are shown in Table 4.16

Table 4.16 Radium-226 content in a standard uranium ore.

Conditions : as summarized in Table 4.14.

Standard Reference uranium ore (NBL 74 A)			Experiment 1			Experiment 2			Average Ra-226 content (Pci)	g Ra / g U	Uranium content found . (g)	Recovery yield for Ra-226 (%)
weight (g)	Uranium content g)	Radium 226 content (Pci)	ingrowth factor	Count rate (cpm)	Ra-226 content (Pci)	ingrowth factor	count rate (cpm)	Ra-226 content (Pci)				
0.1187	$1.23X10^{-4}$	42.3	0.7185	101.1	40.19	0.6628	101.8	43.89	42.04± 2.62	$3.41X10^{-7}$	$1.22X10^{-4}$	99.39
0.2003	$2.09X10^{-4}$	71.5	0.7185	183.6	73.01	0.6628	184.2	70.80	71.9± 1.56	$3.46X10^{-7}$	$2.09X10^{-4}$	100.56
0.3240	$3.36X10^{-4}$	115.6	0.7185	286.2	113.80	0.6628	269.1	115.02	114.91± 1.57	$3.42X10^{-7}$	$3.36X10^{-4}$	99.40
0.4024	$4.18X10^{-4}$	143.8	0.7185	354.1	140.82	0.6628	335.3	144.52	142.67± 2.62	$3.41X10^{-7}$	$4.15X10^{-4}$	99.21
0.5311	$5.52X10^{-4}$	189.9	0.7185	467.6	193.89	0.6628	429.4	185.10	189.50± 6.22	$3.43X10^{-7}$	$5.51X10^{-4}$	99.79

The results indicate that the developed method is very effcitive for the determination of radium-226 contents. If the uranium in the ore is in the radioactive equilibrium with its daughters, the uranium content in the ore could be precisely determined.

4.6 Determination of radium-226 content in monazite samples.

The radium-226 contents in 15 monazite samples were investigated. Analyses were performed at the optimum conditions as described in Table 4.14. The results are given in Table 4.17.

Table 4.17. Radium 226 content in monazite samples.

Conditions : as summarized in Table 4.14

sample	weight (g)	Expt.1			Expt.2			Ra-226 content (experment) ($Pcig^{-1}$ sample)	(1) U-content when equilibrium is assumed	(2) U-content* from delayed neutron analysis	$g_{Ra}/g_{()}$ (delayed)
		ingrowth factor	count rate (cpm)	Ra-226 found ($Pcig^{-1}$)	ingrowth factor	count rate (cpm)	Ra-226 found ($Pcig^{-1}$)				
PG2	3.0039	0.6628	285.0	40.90	0.6628	308.7	44.30	42.30±1.44	0.0127	0.5±0.03	0.09×10^{-7}
	3.0122	0.6628	292.1	41.80	0.6628	294.7	42.18				
PG3	3.0061	0.6628	119.8	17.18	0.6628	99.4	14.25	15.02±1.28	0.0048	0.35±0.02	0.04×10^{-7}
	3.0050	0.6628	116.1	16.65	0.6628	111.4	15.98				
PG 4	3.0070	0.6628	287.1	41.16	0.6628	270.7	38.80	38.58± 2.55	0.0116	0.33±0.02	0.03×10^{-7}
	3.0128	0.6628	245.1	35.07	0.6628	274.5	39.28				
RN1	2.6681	0.7653	103.7	14.51	0.5958	77.8	13.99	13.30±1.22	0.0040	0.38±0.02	0.03×10^{-7}
	3.0045	0.7653	76.0	11.74	0.5958	81.1	12.95				
RN2	3.0615	0.6628	114.0	16.05	0.6628	101.8	14.34	14.82±1.25	0.0045	0.30±0.02	0.05×10^{-7}
	3.0358	0.6628	93.5	13.28	0.6629	109.8	15.59				
RN3	3.0886	0.6628	138.0	19.40	0.6628	125.4	17.50	18.56±0.83	0.0056	0.26±0.02	0.07×10^{-7}
	3.0481	0.6628	129.7	18.34	0.6628	134.4	19.01				
RN4	3.0088	0.6628	215.2	30.97	0.5958	182.0	29.01	30.06±1.36	0.0090	0.25±0.02	0.12×10^{-7}
	3.0065	0.6628	219.5	31.47	0.5958	180.5	28.78				
RN6	3.0248	0.6628	213.0	30.07	0.5958	178.9	28.37	27.07±2.93	0.0081	0.32±0.02	0.08×10^{-7}
	4.0015	0.6628	164.5	23.63	0.5958	162.0	25.89				

Sample	weight (g)	Expt.1			Expt.2			Ra-226 content (experiment) ($Pcig^{-1}$ sample)	U-content when equilibrium is assumed	U-content* from delayed neutron(%)	$\frac{g_{Ra}}{g_U}$ (delayed)
		ingrowth factor	count rate (cpm)	Ra-226 found ($Pcig^{-1}$)	ingrowth factor	count rate (cpm)	Ra-226 found ($Pcig^{-1}$)				
RM8	3.0057	0.6628	193.9	26.38	0.7185	182.5	24.15	24.53±1.80	0.0074	0.30±0.02	0.08×10^{-7}
	3.0063	0.6620	154.8	22.19	0.7185	191.9	25.38				
TK1	2.4985	0.7185	942.2	149.96	0.5958	627.0	120.34	131.57±13.01	0.0396	0.46±0.03	0.29×10^{-7}
	2.7682	0.7185	870.2	125.00	0.5958	756.1	130.98				
TK2	2.9349	0.7185	701.7	95.08	0.5958	592.2	96.76	95.13±2.88	0.0029	0.30±0.02	0.32×10^{-7}
	3.0088	0.7185	788.3	97.57	0.5958	571.6	91.10				
TK3	2.9940	0.5958	36.1	5.78	0.5958	42.2	3.76	6.34±0.41	0.0019	0.26±0.02	0.07×10^{-7}
	3.0010	5.5958	40.1	6.41	0.5958	40.1	6.41				
TK5	2.9951	0.5958	139.8	22.38	0.5958	131.8	21.10	22.80±1.45	0.0069	0.29±0.02	0.08×10^{-7}
	3.0077	0.5958	145.2	23.15	0.5958	154.0	24.56				
TK7	3.0165	0.6628	188.2	26.90	0.7653	230.5	28.53	28.20±1.40	0.0085	0.37±0.02	0.08×10^{-7}
	3.0016	0.6628	190.3	27.33	0.7653	241.4	30.02				
TK8	3.0018	0.6628	419.2	59.91	0.7653	500.5	62.25	61.06±1.23	0.0184	0.89±0.05	0.07×10^{-7}
	3.0112	0.6628	419.7	60.08	0.7653	499.9	61.98				

*Department of Chemistry, the Office of Atomic Energy for Peace.

As already mentioned under section 4.5., if the uranium ore is in radioactive equilibrium, the weight ratio of radium to uranium should be 3.44×10^{-7}. The uranium content in the monazite samples were analyzed by the technique of delay-meutron counting. The results obtained clearly show that the ores are not in equilibrium.